Heat transfer characteristics of an inclined single-phase toroidal thermosyphon

Sh. H. Shams El-Din
Mech. Power Eng. Dept., Faculty of Engineering, Menofiya University, Menofiya, Egypt

An experimental investigation of single- phase liquid in the toroidal thermosyphon inclined at various angles to the horizontal is reported. With water as the filling fluid, the system is studied over a range of low Rayleigh numbers. The study included the effect of heated length- tube diameter ratio, heated- cooled length ratio, diameter of torus- tube diameter ratio and angle of inclination on the heat transfer rate. The data show that both heated length- tube diameter ratio and heated- cooled length ratio have monotonic effect on the heat transfer rate. The effect of torus diameter is to change the heat transfer rate by eleven percent for the thermosyphon considered in the experimental study. The correlations obtained fit the experimental data for all variable parameters adequately. The experimental results obtained from the present study are compared with other results in case of vertical toroidal plane. The comparison is fairly well.

فى هذا البحث تمت دراسة خصائص انتقال الحرارة لمائع أحادى الطور داخل سيفون حرارى حلقى الشكل. يميل على الأفقى عملياً. تمت دراسة تأثير كل من ميل السيفون على الأفقى وتأثير رقم رالى. وكذلك تأثير كل من نسبة طول المبخر إلى طول المكثف ونسبة طول المبخر إلى قطر أنبوب السيفون ونسبة القطر الحلقى للسيفون إلى قطر أنبوب السيفون على معدلات انتقال الحرارة. تبين من الدراسة أن تأثير كل نسبة طول المبخر إلى طول المكثف ونسبة طول المبخر إلى قطر أنبوب السيفون متماثل ويعمل على نقصان معدل انتقال الحرارة بزيادة كل منهما. وكذلك زيادة القطر الحلقى للسيفون يعمل على زيادة معدل انتقال الحرارة فى حدود ١١%. ووجد أيضاً أن أنسب زاوية ميل للسيفون تعطى أكبر معدل الانتقال الحرارة فى حدود ٣٠°- ٤٠°. وتم الحصول على معادلة تجريبية تبين تأثير كل من زاوية ميل السيفون، نسبة طول المبخر إلى قطر أنبوب السيفون ونسبة طول المبخر إلى طول المكثف والقطر الحلقى للسيفون إلى قطر أنبوب السيفون ورقم رالى على قيم رقم ناسلت. وتمت مقارنة النتائج الحالية بنتائج الأبحاث الأخرى فى حالة الوضع الرأسى للسيفون الحرارى وقد وجدت أنها مطابقة مع الآخرين.

Keywords: Natural circulation loop, Thermal expansion, Buoyancy forces, Tororidal, Thermosyphon

1. Introduction

Thermosyphons are devices heated at locations below the points of cooling so that mass and heat transfer around the loop is transported through natural convection processes. For the single-phase thermosyphon and in the presence of gravity, buoyancy forces due to thermal expansion of a working fluid maintain the flow. Thus a circulation is created which transfers energy by convection from the heated section of the loop to the cooled one.

The toroidal thermosyphon consists of a closed loop of tubing in the form of a tours. The tube is filled with a fluid and heated over a part of its length and cooled over the other part.

The steady and time dependent behavior of closed natural circulation loops is important for several engineering applications. For instance, in solar thermosyphon hot water heaters, the heat transfer fluid is heated at the solar collector and rises through a pipe to an elevated storage tank. Here, it transfers heat to the water in the tank, and consequently falls back down to the collector. Natural circulation may also arise in the emergency cooling of nuclear reactor cores, e.g., when a pump failure occurs. Other applications include cooling of internal combustion engines and turbine blades, geothermal power production, thermosyphon reboilers, heat exchanger fins, permafrost protection, ice production, computer cooling, green houses, arctic and climate applications.

A major advantage of these devices is that efficient heat removal is achieved by a flowing fluid without the need for a pump. Flow in a toroidal thermosyphon is driven by buoyancy

forces created by heating and cooling of the internal fluid. The motion of the fluid is opposed by frictional shear forces between the fluid and the wall of the torus. For fixed heat addition and heat removal conditions, the steady-state flow rate in the thermosyphon is the value for which buoyancy and frictional forces are balanced. The circulatory flow is enhanced by larger heat addition rates because the fluid density differences within the thermosyphon are increased.

Most studies on the toroidal loop have considered one of the following modes of heating:

a. Known heating flux over a part of the loop and convective cooling with constant heat transfer coefficient and known wall temperature over the remaining part.

b. Known heating flux over the whole loop.

c. Convective heat transfer with constant coefficient and known wall temperature over the whole loop.

Other treatments have considered the temperature change in the cooling heat exchanger or property variations [1].

Generally speaking, experimental work has approximated heating mode (*a*). Creveling et al. [2] studied the nature of motions in a toroidal thermosyphon oriented in the vertical plane. A constant wall flux inwards for negative angle θ (the lower half of the torus), and constant T_w for positive angle θ. They found that steady flow solutions of the one-dimensional model equations agreed with experiments only if the wall- stress parameterization in terms of the mass flux is varied with the applied heating rate (q). For low heating rates, frictional drag was proportional to q, while at higher values the actual internal motion appeared to be turbulent and the stress seemed to follow a $q^{1.5}$ law. Using these friction laws they computed the stability of the predicted steady flows by deriving a transcendental characteristic equation for the linear growth rates that had an infinite number of roots. The stability results gave partial agreement with experiments. Damerell and Schoenhals [3] studied the predicted and observed steady flow in a toroidal thermosyphon with angular displacement of heated and cooled sections. A one- dimensional, steady- state analysis predicted that the mass flow rate would decrease monotonically with increasing the tilt angle. However, it was found experimentally that for small tilt angles, the flow rate did not vary significantly with tilt angle. The discrepancy was attributed to the regions of streamwise flow reversal which were once again observed near the entrance to the cooling section. Good agreement was obtained between analytical predictions and measurements for large values of the angular displacement of the heated and cooled sections. Greif et al. [4] integrated the one- dimensional thermosyphon model with linear drag using a finite- difference representation in the angle θ to obtain further information about the predicted transient behavior of the simple loop. These two studies have been extended to other situations of practical importance. Mertol et al. [5] studied the transient daytime and night time performance of a thermosyphon solar water heater with a heat exchanger in the storage tank. It was found analytically that the flow reverses during the night but the magnitude of the reverse flow is reduced when high viscosity fluids, such as propylene glycol are used. It was also observed that low viscosity fluids have strong oscillations during the night. Mertol et al. [6] analyzed the steady- state, transient and stability behavior of a toroidal loop. The loop was oriented in a vertical plane which is heated over the lower half and cooled by maintaining a constant wall temperature on the upper half. The conservation equations were averaged over the cross section and an analytical solution was derived for the steady state condition. A numerical method was used to obtain the transient flow and heat transfer by solving simultaneously the momentum and energy equations. The results include stable, as well as unstable, configurations and also revealed multiple solutions. Mertol et al. [1] studied the heat transfer and fluid flow in a natural convection loop. This study was concerned with the transient, steady-state, and stability behavior of a toroidal thermosyphon. The thermosyhon is heated over the lower half and cooled over the upper half by an annular parallel flow heat exchanger. The results include the efficiency of the heat exchanger and the pressure drop along the heat exchanger as well as the detailed temperature distributions and velocity variations. Studies have been car-

ried out for stable and for unstable conditions. Hart [7] tackled a general heating flux, including heating mode (a), under certain symmetry conditions. His assumption of symmetry, not only in the heating flux but also in the temperature field, permitted him to decouple three "master" equations from the rest. The basic assumption of temperature symmetry is, however, difficult to justify since numerical calculations [4] show distinct asymmetry about a vertical diameter even if the heating is symmetrical. The mass flux is determined solely by the master problem. In the strongly non- linear regime, it is argued that only steady or chaotic flows, not periodic ones, are possible. The sensitivity of the one-dimensional model predictions to various wall-stress parameterizations is described. Mertol et al. [8] studied the steady-state and transient pressure variation in a closed toroidal natural convection loop. This work differs from previous studies by introducing the pressure distribution in the analysis. Limiting analytical expressions have also been derived for the steady-state pressure distributions. The results showed that the static pressure is up to four orders of magnitude greater than the dynamic pressure. Therefore, the total pressure is essentially hydrostatic. Sen et al. [9] studied the behavior of a toroidal thermosyphon with known heat flux around the loop. Criteria were first established for steady-state solutions. The transient governing equations were then transformed to an infinite set of ordinary differential equations. The flow velocity was determined from a set of three equations which decouple from the rest. The existence and stability of the critical points of these equations were examined, and typical numerical solutions for different values of the governing parameters were presented. Chaotic solutions were shown to be possible. Theoretical analysis on the inclined toroidal loop has been made by Sen et al. [10] in order to obtain an exact expression for the steady-state velocity. The analysis was devoted to a torodial geometry which is heated with constant heat input over a half of its length and cooled by means of a heat exchanger with constant heat transfer coefficient (h) and wall temperature T_w on the other half. The heated and cooled sections were inclined at an angle θ with respect to the horizontal plane. The results demonstrated that the flow can have zero, one, two, or three steady-state velocities. It was found also that the maximum velocity is not always attained for zero angle of inclination. Experiments performed on the studied geometry confirmed the salient features of the one-dimensional analysis, especially regarding the velocity-inclination diagram. In particular, stable steady-state velocities have been observed in all four quadrants of the diagram. Lavine et al. [11] performed a three dimensional analysis of the toroidal thermosyphon, with all velocity components included. The results confirmed the experimental observations of three dimensionality, streamwise flow reversal, and secondary motion. Regions of streamwise flow reversal were predicted for cases of low tilt angle. It has been concluded that the flow reversals reduced the wall friction and buoyancy forces, and consequently have a strong effect on the average axial velocity.

There are important differences in the one-dimensional modeling of thermosyphons with single and multiple loops. This has been discussed by Sen and Fernandez [12] for a general configuration of tubes having arbitrary shape starting from one point and ending at another. For single loops, either axially heat-conduction or axially non-heat-conduction energy equations can be used. However, for the problem of (n) branches starting from one point and meeting at another, two important special cases can be treated using the conductive or non-conductive model. The effect of small differences between seemingly identical branches on the steady-state operation of the thermosyphon has yet to be fully determined. Sen et al. [13] studied the steady-state natural convection in a toroidal loop with a heated diametrical branch and cooled side branches. The loop was rotated to vary the tilt angle of the diametrical branch. A one dimensional analysis was carried out to provide the fluid velocities and temperature distributions in the loop. The effect of axial conduction was examined. It was reported that, with increasing tilt angle from the vertical, the fluid in the lower side branch slows down and reverses. The flow through the central branch increases and the return path is through the upper side branch. For small tilt angles around the horizontal,

multiple steady states exist. Comparison of experiments on a water filled glass loop was in qualitative agreement with the analysis and multiple steady states are observed.

The purpose of the present study is to investigate the variation in steady flow rate of the closed toroidal thermosyphon for inclinations ranging from the vertical to the horizontal. The study is restricted to low Rayliegh numbers. A toroidal geometry is heated over different sections of its area and cooled over the remaining area of the loop. The effects of fluid properties, system dimensions and heat transfer rate on the Nusselt number have been thoroughly discussed. The comparison between the results obtained from the present study and previous investigation is also made.

2. Analysis

For single-phase thermosyphons the steady- state, one-dimensional models are considered. The closed loop has a torus shape with a prescribed circular cross sectional area.

Mass conservation in the loop indicates that:

$$\rho u A = \dot{m} = const. \tag{1}$$

The momentum balance equation in the loop can be written as:

$$\rho u \frac{du}{dx} = -\frac{dP}{dx} - k_f u - g\rho . \tag{2}$$

The term on the LHS of the equation represents an inertia force while those on the RHS are the pressure, frictional and gravity forces, respectively. In eq. (2) we have assumed that the frictional force is a linear function of the velocity, thus we have:

$$k_f = \frac{8\pi\mu}{A} . \tag{3}$$

The one- dimensional energy equation takes the form:

$$\dot{m} \frac{d(i + u^2/2)}{dx} = q_L - \dot{m} g . \tag{4}$$

Where i is the fluid specific enthalpy and q_L is the heat inflow per unit length along the loop. Using eqs. (1) and (2), and the definition of enthalpy $i = e + P/\rho$, the energy equation can be conveniently written as:

$$\dot{m} \frac{de}{dx} = q_L + \frac{uAP}{\rho} \frac{d\rho}{dx} + A k_f u^2 . \tag{5}$$

The first term on the RHS indicates that the fluid internal energy changes due to external heat sources or sinks. The second and third can be identified with the internal energy changes due to pressure work and viscous dissipation respectively. One must observe that the integral of the energy eq. (4), over the entire loop gives:

$$\int_0^L q_L(x) dx = 0.. \tag{6}$$

Which merely indicates that for a steady-state solution to be possible, the total heat input in the system must balance the heat output.

We consider the Boussinesq approximation in which the fluid properties are assumed constant except for the body force term where we will consider a linear variation of the density with temperature:

$$\rho = \rho_o [1 - \beta (T - T_o)]. \tag{7}$$

Here ρ_o the density at a reference temperature T_o, taken to be that at $x=0$.

The momentum eq. (2) reduces to:

$$\rho u \frac{du}{dx} = -\frac{dp}{dx} - k_f u - g\rho_o \left[1 - \beta (T - T_o)\right]. \tag{8}$$

We will consider that viscous dissipation and compressibility effects are negligible compared to the heat input, so that energy eq. (5) becomes:

$$\dot{m} c \frac{dT}{dx} = q_L . \tag{9}$$

Where we have considered $e = cT$. From this equation:

$$T = T_o + \frac{1}{\dot{m}c}\int_0^X q_L(\bar{x})d\bar{x}\,. \qquad (10)$$

Integrating eq. (8) around the loop, we have:

$$\int_o^L k_f u dx = \beta\rho_o \int_0^L gT dx\,. \qquad (11)$$

It should be noticed that the integral of the inertia force is zero. Substituting eqs. (1), (3) and (10) into (11) leads to the following expression for the mass flow rate:

$$\dot{m} = \pm\left[\frac{\beta\rho_o^2 A^2}{8\pi c\mu L}\int_0^L g(x)\left(\int_0^x q_L(\bar{x})d\bar{x}\right)dx\right]^{1/2}. \qquad (12)$$

Depending on the value of the integral term;

$$I = \int_0^L g(x)\left(\int_0^x q_L(\bar{x})d\bar{x}\right)dx\,,$$

two distinct steady - state solutions are possible. For $I<0$, no real solutions exist but the real solutions exist when $I > 0$, which indicates that the heating section should be at a lower position than the cooling section for the steady-state solution to exist.

3. Experimental considerations

3.1. The test rig and instrumentation

A schematic diagram of the experimental apparatus is shown in fig. 1. The thermosyphon was fabricated from a copper tube in the form of a torus with a major diameter of 63 cm and a constant minor diameter of 1.96 cm. It was filled with distilled water. The lower section of the toroidal thermosyphon was heated electrically using resistive tape. A layer of fiberglass tape is wrapped around the outer surface of the torus before the heating element is positioned. To study the effect of heated-cooled length ratio (L_h/L_c) and heated length-diameter of tube ratio (L_h/d) on the heat transfer rate, the heated length is changed by winding the heater at different lengths of 27, 36, 63, 87 and 99 cm of the torus length.

Electric power was supplied to the heater through a variable transformer. The power delivered to the heater was measured using a voltmeter and an ammeter simultaneously.

Power input values ranged from 30 to 180 Watts for the experiments. The heated portion of the torus was wrapped on the outside with insulation to minimize heat losses to the surroundings.

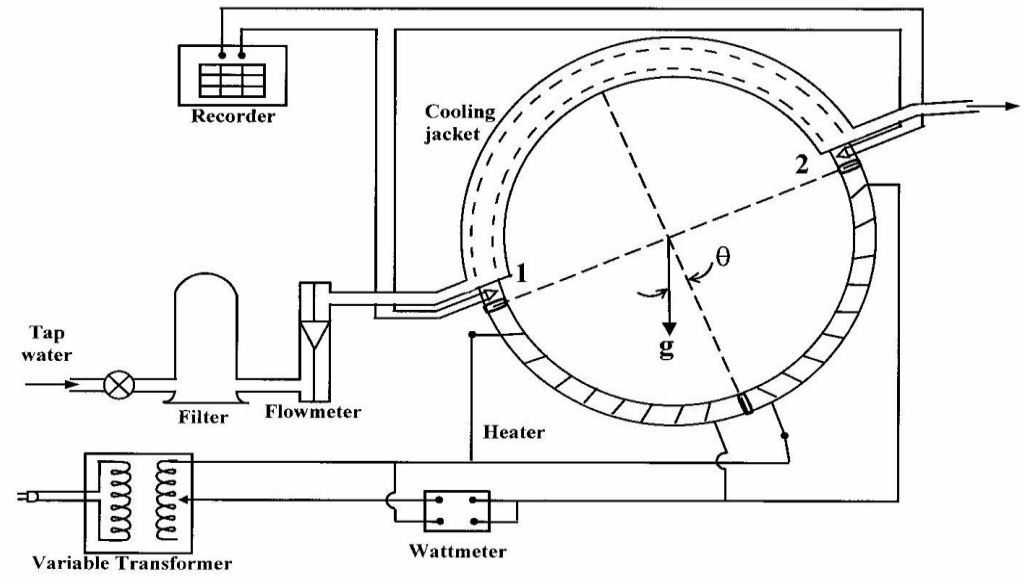

Fig. 1. Schematic diagram of experimental apparatus.

Heat was removed by an annular cooling jacket which surrounded the remaining portion of the torus. Filtered tap water was used as the coolant fluid. The tap water flow rate was measured, and temperature at both the inlet and the outlet of the cooling jacket was measured. Since the temperature of the tap water was very close to ambient room temperature. By insuring that the flow rate of cooling water was much greater than the flow rate of the water inside the thermosyphon, a close approximation to constant wall temperature cooling was provided. Under these conditions, the temperature change experienced by the coolant, while passing through the jacket, was much smaller than the temperature change experienced by the internal fluid as it is passed through this section. Two Chromel–Alumel thermocouples were installed inside the thermosyphon to measure the temperatures at the two locations just upstream and downstream of the heated section to know the maximum power added before the water is turned into vapour. Using these measured temperatures, the measured power input and the known specific heat of the internal fluid, the flow rate for the thermosyphon was calculated from an energy balance for each test run in which the flow was steady. Measurements of heat input and temperatures at locations just upstream and downstream of the heated section were made by using precise instruments with adequate accuracy (Within ±5 percent).

To measure the wall temperatures along the toroidal thermosyphon (for heated and cooled portions) the twenty two Chromel- Alumel thermocouples were fixed on the surface of torus.

To study the effect of the torus diameter on the heat transfer rate, different torus have been made from copper tubes with the same internal diameter 1.96 cm and different diameters of torus of 30,34, and 55 cm.

To provide inclination of the torus, the entire apparatus has been mounted on a stand provided with cylindrical hinges. The stand enables the inclination angle to be adjusted to the desired value measured from the horizontal. This arrangement provided a very convenient cooling system for the upper section of torus which could thereby be studied at any inclination between the vertical and the horizontal.

Temperature has been measured at various locations by means of thermocouples located inside the torus and along the thermosyphon heated and cooled sections walls at intervals of 9 cm a part. The torus thermocouples were installed on the outside of the wall before they have been wrapped with the fiberglass tape. The wires have been led out along insulated sleeves wherever possible and have been connected to a digital millivoltameter via a switching box.

During the tests, adjustments in the power being supplied to the heater made it possible to control the axial variation in tube wall temperature. Prior to the tests, the heated section was calibrated in order to determine its heat loss which had to be subtracted from the gross electrical power being supplied. The heated and cooled sections have been insulated with glass wool (5 cm thick, k= 0.04 W/m k). The mass flow rate of the cooling water has been measured with a calibrated flowmeter. The flow rate has been fixed at a sufficient value to insure a fairly uniform tube wall temperature both circumferentially and axially. No attempt has been made to estimate the heat lost from the cooled section by convection, since it was assumed to be equal to the net heat supplied to the heated section under the steady conditions studied.

3.2. Procedure and test schedule

After the calibration runs, experiments have been conducted as follows. The water is forced through an annular cooling jacket which surrounds the cooled section. The temperatures are set to the predetermined values. The tube heaters are switched on and the power is set at some level within the anticipated range of the run (30- 180 Watt). Pipe temperatures at various locations on both the heated and cooled sections are then monitored and adjusted periodically in order to obtain an acceptable degree of uniformity. Then the system was allowed to operate under such fixed conditions for a sufficiently long time period to allow transient effects to fade out. This procedure was continued for a period of 1-2 hours by the end of which the system reaches a

steady-state condition. For each experiment the heat input, cooling water flow rate and tilt angle of the heated and cooled sections were adjusted to prescribed values.

When all readings attain satisfactory steadiness and the values were recorded, the power level was then altered and the procedure was repeated, without changing the coolant water conditions. At the end of a run, the entire system was shut down and the thermosyphon torus is either exchanged or modified for the next run. Modifications included changes in heated length, cooled length, diameter of torus or inclination angle. For each data point, the local wall temperatures have been used to calculate an average value for the heated and cooled pipe wall temperatures, these values have been then used to calculate the total heat transfer coefficient as follows:

$$q_a = \frac{Q}{\pi d_i L_h}, \tag{13}$$

and

$$Nu = \frac{h.d_i}{K} = \frac{Q}{\pi k L_h (\bar{T}_h - \bar{T}_c)} . \tag{14}$$

4. Results and discussion

The heat transfer characteristics of inclined torodial thermosyphon are shown in fig. 2. The experimental data presented fall in the low range of Rayleigh number where slowly varying Nusselt number behaviour is found to decrease abruptly at the low end. It is noticed that increasing T_d would increase the effective Nusselt number. For high Ra the slope of the Nu- T_d curves tend to decrease. For small values of Ra, the variation of slope is attributed to radial temperature gradient which is steep near the wall and shallow in the interior regions occupied by the returning core. The axial temperature gradient steepens as the points of intersection between the heating and cooling sections are approached, where it attains a maximum. The magnitude of the maximum value increases with the tube radius. At the wall, the axial temperature gradient reaches its greatest value. Therefore, near the wall the presence of a thermal instability is felt first and has a strong effect.

In the absence of a thermal instability, the fluid would tend to a purely refluent system, the heat transfer between the two sections is then mainly by conduction across the junction plane. It is hypothesized that such a coupling mechanism would continue until a critical (transitional) value of Ra^* has been attained. For $Ra > Ra^*$, the lower (hot) annulus of rising fluid must somehow cross through the upper (cold) descending fluid, and vice versa. This advective breakthrough occurs at a value of Ra much greater than the value associated with convective turnover. Equally important is the fact that the advective mechansim will be associated with a secondary mixing process, the vigour of which will depend upon Ra and the size of the region within which the advective process occurs. The presence of advective process improves the heat exchange by conduction. But, secondary mixing can be expected to have a deleterious effect. These two opposing effects cancel each other and thereby render the overall Nusselt number essentially independent of Ra, at least up to 10^6. However, for $Ra \leq 10^5$ in shorter cavities, the flow field may not be unique, or at least its marked tortuosity may be very sensitive either to the intial conditions of the experiment or to the boundary conditions. Thus, small temperature fluctuations, or imposing slightly different heat and cooling arrangements, may have been sufficient to create a stable flow. This is particularly true near the junction region. Consequently, the heat transfer rate is changed dramatically. Further, it could be suggested that thickest point of the boundary layer interfere with narrowest point of core resulting in destabilization of the flow. The flow exhibits unstructured motion, which creates a choking stagnation mechanism. The motion of the flow is reestablished in either the impeded or laminar regime. The global circulation is upwards over the heated and cooled wall and is downwards along the core. This circulation would be partially reversed due to the choking stagnation, should this situation prevails at low Ra, the rate of heat transfer declines rapidly.

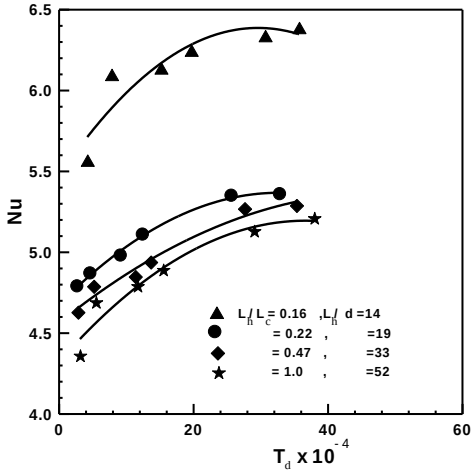

α= 30°

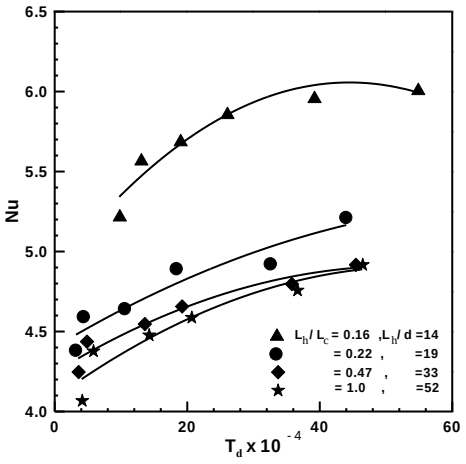

α= 60°

(a) D/d= 33

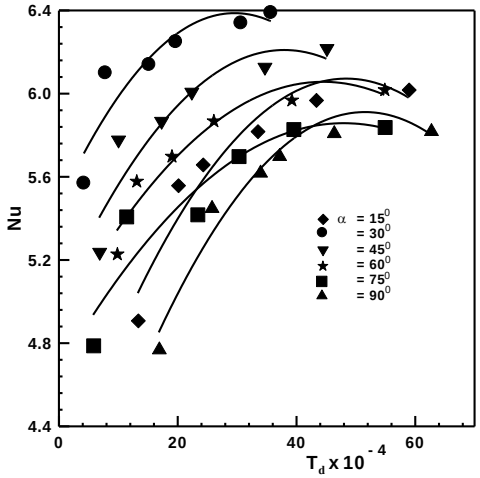

L_h/L_c= 0.16, L_h/d= 14

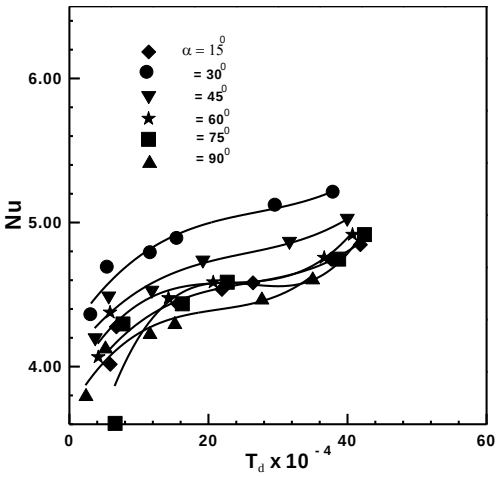

L_h/L_c= 1, L_h/d= 52

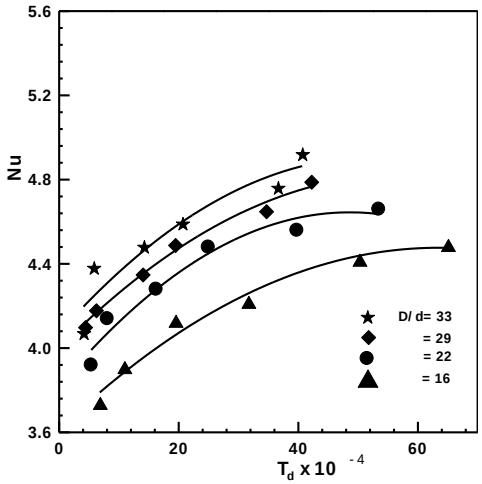

α= 60°, L_h/L_c= 1

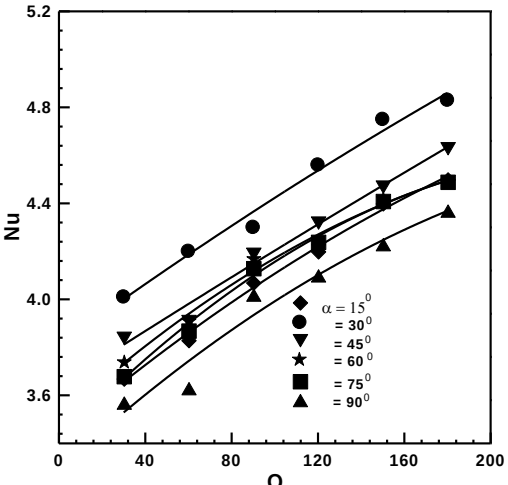

L_h/L_c= 1

Fig. 2. Variation of heat transfer rate with Rayleigh number.

4.1. Effect of geometry

The effect of geometry on the heat transfer performance of the toroidal thermosyphon has been investigated at low Rayleigh numbers. Fig. 2 reveals that torus geometry has a significant effect on the location of transitional regime. This dependency would be expected if the transition spanned only a narrow range of Ra, essentially determined by the low Rayleigh number range.

The effect of heated- cooled length ratio L_h/L_c is shown in fig. 3. Whenever this ratio departs from unity the longitudinal symmetry of the system is lost and the flow system in the upper and lower sections will no longer be mirror images. For any given heat flux, the thickness of the annular stream and core, in each section, will generally be different across the junction plane, thus, altering the details of the coupling process in accord with the torus geometry. Such changes must be compatible with corresponding changes in the flow system deep within each section. As L_h/L_c is decreased from the limiting value, the rate of conduction increases as the cooled pipe surface increases, but it is not until an adjective breakthrough occurs that the thermal exchange mechanism and the corresponding heat transfer efficiency change significantly. An increase in L_h/L_c may thus be viewed as a tendency towards increasingly refluent behavior, thereby increasing the overall thermal impedance of the system. This reduction in performance is detectable in fig. 3. It appears from the figure that the greater the increase in L_h/L_c, the greater is the reduction in heat transfer.

The effect of heated length- diameter ratio L_h/d on heat transfer is much greater than the effect of heated- cooled length ratio L_h/L_c, exhibited in two ways. Firstly, the location of the transitional T_d range is lowered as L_h/d increases, this is consistent with the proposed effect on inversion. Secondly, the Nusselt number is decreased as L_h/d is increased, again in accord with the suggested coupling processes. These monotonic effects are in accord with previous studies of the closed tube thermosyphon.

The effect of diameter of torus on the heat transfer performance is shown in fig.4. It is noticed that, the heat transfer rate increases with the increase of torus diameter and the percentage of change is equal to eleven percent in the range of diameter change of the torus (30-63 cm). This is attributed to that the transition is more likely to occur in the laminar boundary layer regime for small diameter of torus D. Whereas in large D, the transition may occur in the laminar impeded regime. Moreover, for small D, the operating temperature difference within the thermosyphon loop, which is the difference between the maximum and minimum temperatures, is small compared to the temperature difference between the loop fluid and the heat exchanger fluid.

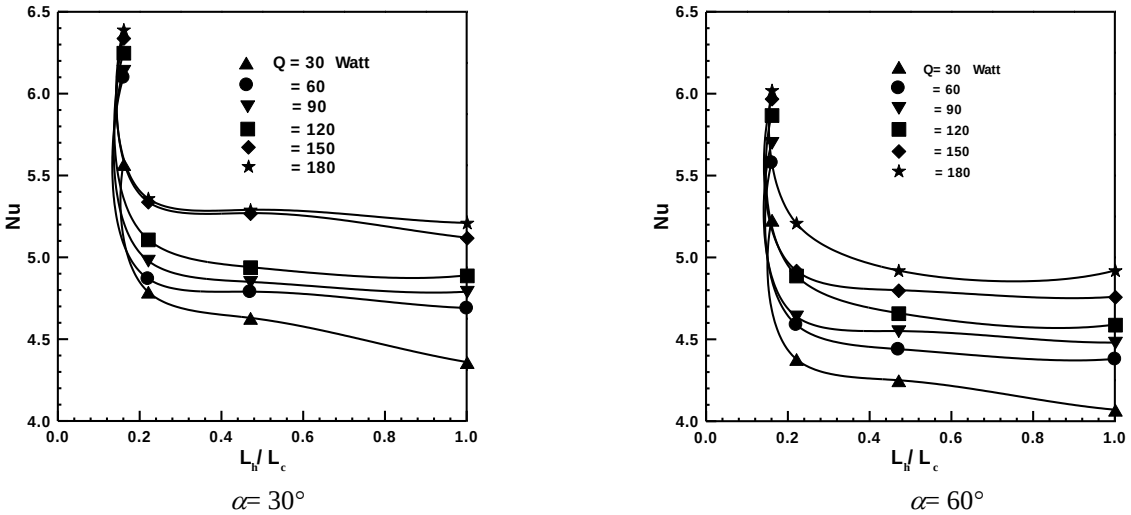

α= 30° α= 60°

Fig. 3. Effect of heat-cooled length ratio on heat transfer rate at D/d= 33.

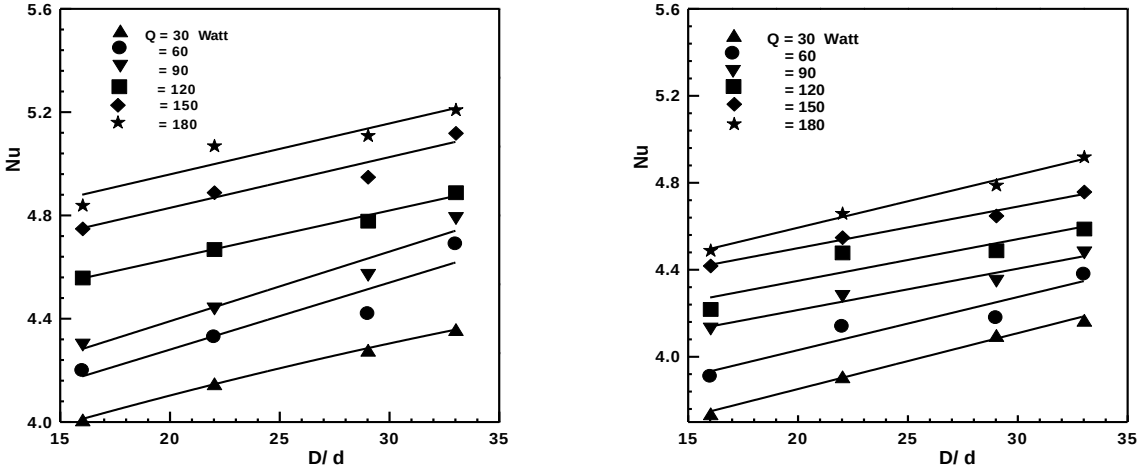

α= 30° α= 60°

Fig. 4. Effect of diameter of torus on heat transfer rate at L_h/L_c= 1.

As D decreases, the temperature differences between the loop and the exchanger fluid increases. This leads to two opposing processes. The first of then is the increase in buoyancy forces which is proportional to the operating temperature difference. The second is the enhanced production of hot and cold pockets inside the loop. Thus, as D decreases, the ratio of the operating temperature difference to the destabilizing temperature difference decreases, which leads to a more unstable system.

The larger the diameter D is the system becomes more stable. As cooling becomes more efficient, the operating temperature difference now increases while the destabilizing temperature difference decreases. This results in a more stable system.

4.2. Effect of inclination

The heat transfer characteristics of inclined torus are shown in fig. 5. The main effect of inclination is to raise the heat transfer rates above the value obtained for a vertical plane. This is seen more clearly by using the smooth curves drawn through the Nu- T_d data to construct cross plots. It is immediately obvious that the heat transfer efficiency initially increases with inclination from the vertical, a trend which appears to be counter intuitive because the longitudinal component of the body force field driving the system decreases with increasing inclination. However, the effective body force field has two components, both of which are evidently important in amounts which vary with inclination.

It is to be expected that as the torus is inclined from the vertical, the initial effect under laminar conditions would be complex but slight. The annular refluent zones would shrink slightly as the two -filament coupling mechanism evolved. These filaments would be subject increasingly to the organizing influence of a component of gravity acting normal to the tube axis, that is, secondary motion would appear. Opposing the gain attributable to a secondary motion is the decrease in longitudinal buoyancy. Overall, the increase in heat transfer rate is small, and slightly nonlinear, this is consistent with previous observations [14,15] which were, however, believed to be for boundary layer conditions. It is suggested that a more plausible explanation follows from the assumption that the near vertical data were mostly in a turbulent impeded regime extending down to the lowest values of T_d where transition to a laminar impeded regime occurs. This assumption accounts for Nusselt number which is low and almost constant.

For inclinations greater than 45° the situation changes substantially as fig. 5 reveals. The extent of the annular refluent zone would be further reduced, but it is believed that this is not the main cause of the rapidly increasing

Nusselt number evident between 45° and 60° with respect to a vertical plane. Normal to the tube axis, g sinα increases with inclination increases with respect to a vertical plane, giving rise to a vigorous secondary circulation in the form of a vortex pair in each filament [16,17]. This evertive augmentation is evidently the cause of the significant rise in heat transfer for α between 45° and 60°. It is also evident that this secondary motion will continue to increase in strength as the inclination increases further. However, the longitudinal component of gravity g cosα continues to decrease as the horizontal position is approached. The primary flow is thus driven by a weakening field which is eventually replaced by the much smaller indirect buoyancy effect dependent upon the horizontal temperature gradient. The opposition of a strengthening secondary flow and a weakening primary flow results in the maximum displayed in fig. 5. Beyond the maximum, the strength of the primary circulation is diminishing which causes the decrease in heat transfer rate.

When the torus is horizontal, annular refluence ceases to exist and the system consists simply of a horizontally driven, two – filament primary loop superimposed on which is a vertically- driven secondary flow consisting of two pairs of longitudinal vortices with opposite signs, and one above the other [16,17]. The primary circulation does not change significantly over a wide range of inclinations near the horizontal [17], this therefore corresponds to a transitional shift from the near-vertical value to a new value valid for large inclinations and determined from the near horizontal flow field. The transition was always steeper than expected because the lowest points were taken with the cooled section wall temperature below the inversion temperature but this did not appear to alter the distinction between the low and high α transitions.

The correlation equation obtained fit the experimental data for all variable parameters. The empirical correlation equation is in the form:

$$Nu = A_o(Sin\,\alpha)^{A1}\left(\frac{L_h}{d}\right)^{A2}\left(\frac{L_h}{L_c}\right)^{A3}\left(\frac{D}{d}\right)^{A4} T_d{}^{A5} \quad (15)$$

The correlation is valid in the range: $\pi/12 \le \alpha \le \pi/2$, $14 \le \frac{L_h}{d} \le 52$, $0.16 \le \frac{L_h}{L_c} \le 1.0$, $16 \le \frac{D}{d} \le 33$ and $10^5 \le T_d \le 10^7$. The standard deviation is within the experimental error of ± 8%. This fit gives:

$$Nu = 1.106\,(0.7 - 1.1\,(sin\alpha)^2 + 1.2\,sin\alpha)^{0.246}\left(\frac{L_h}{d}\right)^{-0.1126}\left(\frac{L_h}{L_c}\right)^{-0.027}\left(\frac{D}{d}\right)^{0.291} T_d{}^{0.07} \quad (16)$$

It is noticed that the exponents in the previous equation reflect the substantially increased influence of torus geometry in defining the coupling mechanism in the laminar boundary layer regime.

The comparison between the present experimental data and the previous results obtained with a vertical plane is shown in fig. 6. It is seen from the figure that the present results are in agreement with other experimental data. The four sets of experimental data shown in fig. 6 were obtained over essentially the same temperature range between 0-100°C and therefore (T_h-T_c) is not significantly different among them. As indicated, they were all obtained with L_h/L_c = 1.0 and $3.75 < L_h/d \le 52$. Most of the data shown in fig. 6 are in the range of $10^5 \le T_d \le 10^7$. The existence of a scale of turbulence comparable with the smaller tube diameter used here may explain the departure from previously observed boundary layer behavior seen in fig. 6.

Fig. 7 shows the present data compared with other previous data at different Raleigh numbers and different inclination angles. It is noticed that, the main flow which occurs in a vertical plane is thus modified to account for the secondary motion. In the coupling region, the model accommodates the effect of thermal buoyancy as the source of a pattern of interlaced streams, or filaments, which cross through each other. In this way it is possible to account for the influence of both the advective and refluence mechanisms, the balance between them determines the overall efficiency of the system.

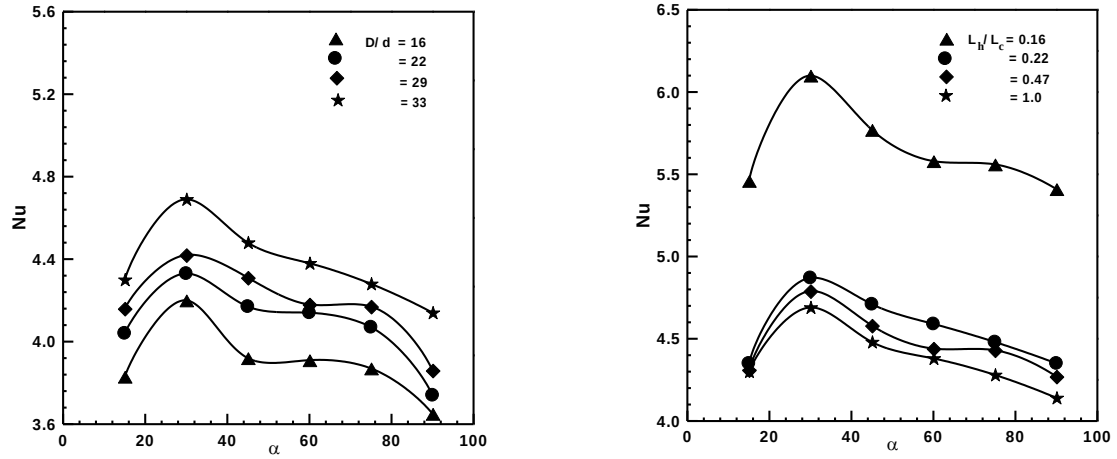

Q= 60 watt

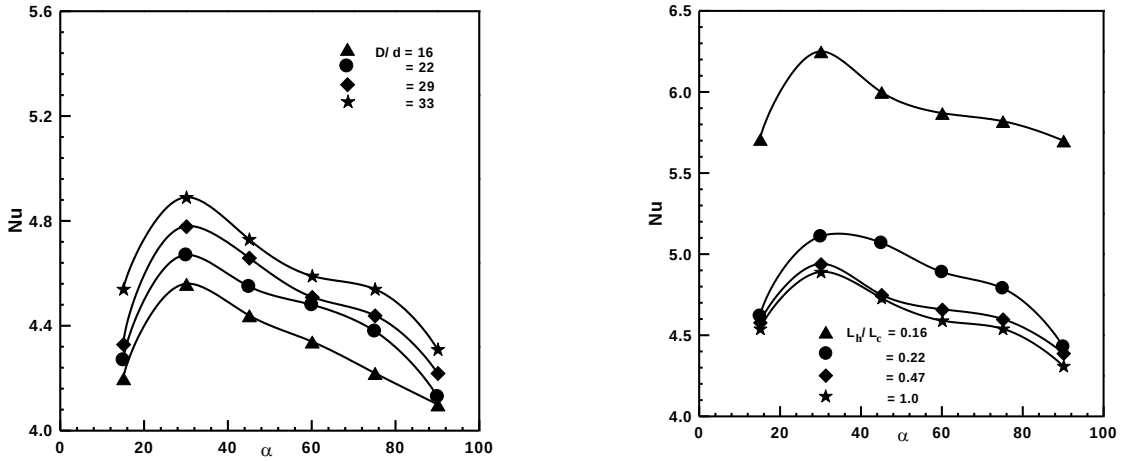

Q= 120 watt

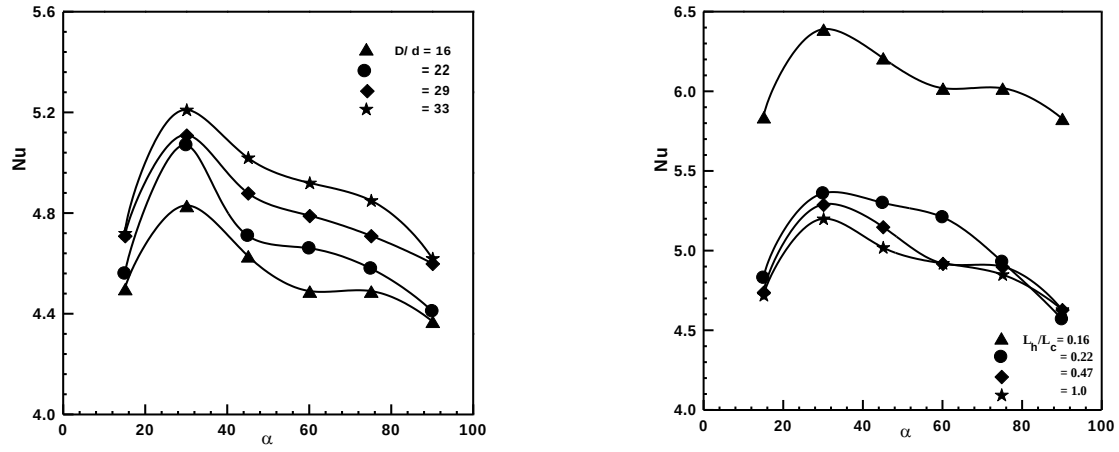

Q= 180 watt

(a) L_h/L_c= 1 (b) *D/d*= 33

Fig. 5. Effect of inclination angle on heat transfer rate.

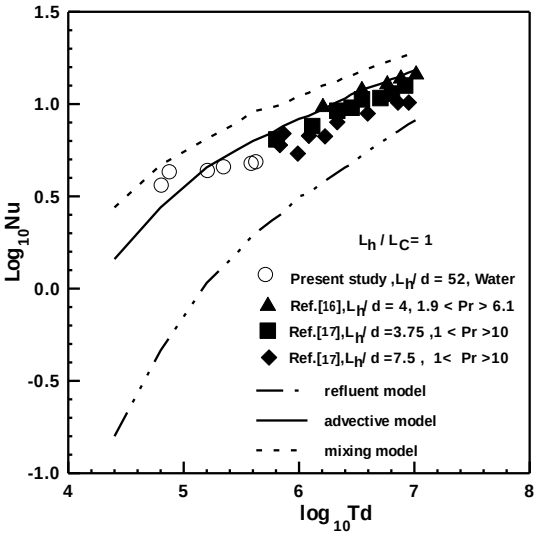

Fig. 6. Comparison with other work with a vertical plane.

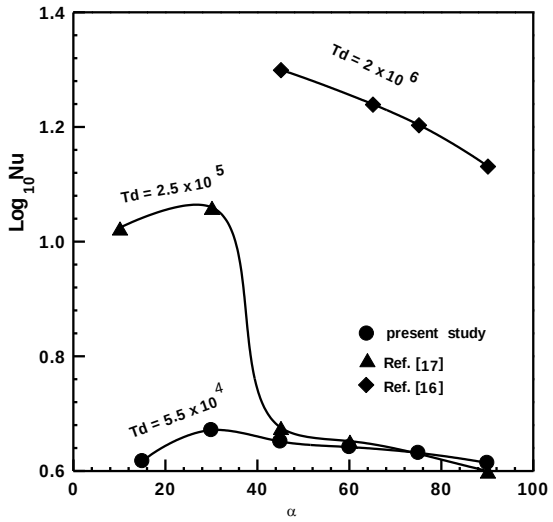

Fig. 7. Comparison with other work at different inclination angles.

Near the vertical position, the flow system may be more complex than two-filament flow. One suggestion is that multi- filament coupling may then exist, the flow pattern may not be unique, thus leading to the possibility of branching in the heat transfer rate. Alternatively, a turbulent impeded regime may have been entered. In any event, the results suggest the gradual emergence of a more efficient two filament flow which accompanies increasing inclination and more than offsets the effect of a decrease in the longitudinal component of the gravitational filed.

For greater inclinations, the flow model was found to be very helpful in interpreting the heat transfer data. In particular, it suggests that further increases in the heat transfer rate are attributable to the increasing evertive augmentation associated with secondary circulation in each of the two filaments. It also provides an explanation of the maximum. Beyond this point, any further increase in secondary motion is more than offset by the decrease in the primary circulation. Eventually, This circulation is driven mainly by the weak effect of horizontal temperature gradients. Then the heat transfer rate decreases.

5. Conclusions

The experimental results of this study have revealed some interesting and important characteristics of the flow and heat transfer in a toroidal thermosyphon. The most significant of these are:

1- The effect of heated length- tube diameter ratio and heated- cooled lengh ratio is monotonic on the heat transfer rate.

2- The heat transfer rate decreases with increasing both of heated- cooled length ratio and heated length- tube diameter ratio.

3- The heat transfer rate increases with torus diameter increase.

4- The maximum heat transfer rate is obtained in the range of 30°-45° of inclination angles to horizontal plane.

5- A correlation equation is obtained for all variable parameters.

6- The comparison of the present data with the previous data is fairly well.

Nomenclature

A cross- sectional area, m^2,
c specific heat, J/kg. K,
d diameter of tube, m,
D diameter of torus, m,
e specific internal energy, J/kg,
g gravitational acceleration, m/sec^2,
h heat transfer coefficient, $W/m^2.K$,
i specific enthalpy, J/kg,
K_f proportionality factor for the frictional force, kg/m^3. sec,
K thermal conductivity, W/m.K,
L tube length of the loop, m,

$\dot{m}$ mass flux, kg/sec,
P pressure, Pa,
Q heat transfer rate, W,
q_a heat per unit area , W/m^2,
q_L heat per unit length, W/m,
T temperature, K,
U longitudinal velocity, and m/sec, and
X longitudinal coordinate.

Greek symbols

α inclination angle rad,
β thermal expansion coefficient 1/K,
μ dynamic viscosity Pa. sec,
ν momentum diffusivity m^2/sec,
ρ density kg/m^3, and
θ diametrical tilt angle rad.

Subscripts

c cooled,
d based on diameter,
h heated,
i internal, and
o refernce state.

Superscripts

- mean, and
* transitional.

Dimensionless groups

$\frac{D}{d}$ torus- tube diameter ratio,

$\frac{L_h}{d}$ heated length- tube diameter ratio,

$\frac{L_h}{L_c}$ heated – cooled length ratio,

Nu Nusselt number $\frac{h.d}{k}$,

Ra Rayleigh number $\rho\beta g\, c(t_h\text{-}t_c)d^3/\nu K$,
T_d $Ra.\, d/L_h$,

References

[1] A. Metrol, R. Greif, and A.T. Giz, "The Trasient, Steady State and Stability Behavior of a Toroidal Thermosyphon with Parallel Flow Heat Exchanger", J. Solar Energy Engng, ASME, Vol. 105, pp. 58-65 (1983).

[2] H.F. Creveling, J.F. De Paz, J.Y. Baladi, and R.J. Schoenhals, "Stability Characteristics of a single – Pahse Free convection Loop," J. Fluid 67, pp. 65-84 (1975).

[3] P.S. Damerell, and R.J. Schoenhals, "Flow in a Toroidal Thermosyphon with Angular Displacement of Heated and Cooled Sections," J. Heat Transfer, ASME, Vol. 101, pp. 672-675 (1979).

[4] R. Greif, Y. Zvirin, and A. Metrol, "The Transient and Stability Behavior of a Natural Circulation Loop," J. Heat Transfer, ASME, Vol. 101, pp. 684-688 (1979).

[5] A. Metrol, W. Place, T. Webster, and R. Greif, "Detailed Loop Model (DLM) Analysis of Liquid Solar Thermsyphons with Heat Exchangers,". J. solar Energy, Vol. 27, pp. 367-386 (1981).

[6] A. Mertol, R. Greif, and Y. Zvirin, "The Transient, Steady State and Stability Behavior of a Thermosyphon with Throughflow," Int. J. Heat Mass Transfer, Vol. 24, pp. 621-633 (1981).

[7] J.E. Hart, "A New Analysis of the Closed Loop Thermosyphon," Int. J. Heat Mass Transfer, Vol. 27 (1), pp. 125-136 (1984).

[8] A. Mertol, A. Lavine, and R. Greif, "A Study of the Variation of the Pressure in a Natural Circulation Loop," Int. J. Heat Mass Transfer, Vol. 27 (4), pp. 626-630 (1984).

[9] M. Sen, E. Ramos, and C. Trevino, "the Toroidal Thermosyphon with Known Heat Flux," Int. J. Heat Mass Transfer, Vol. 28 (1), pp. 219-233 (1985).

[10] M. Sen, E. Ramos and C. Trevino, "On the Steady- State Velocity of the Inclined Torodial Thermosyphon," J. Heat Transfer, ASME, Vol. 107, pp. 974-977 (1985).

[11] A.S. Lavine, R. Greif, and J.A.C. Humphrey, "three. Dimensional Analysis of Natural Convection in a Torodial Loop: Effect of Tilt Angle," ASME, J. Heat Transfer, Vol. 108, pp. 796-805 (1986).

[12] M. Sen, and J.L. Fernandez, "One Dimensional Modeling of Multiple- Loop Thermosyphons", Ine. J. Heat Mass Transfer, Vol. 28 (9), pp. 1788-1790 (1985).

[13] M. Sen, D.A. Pruzan, and K.E. Torrance, "Analytical and Experimental Study of Steady-State Convection in a Double-Loop Thermosyphon," Int. J. Heat Mass Transfer, Vol. 31 (4), pp. 709- 722 (1988).
[14] D. Japikse, P.A. Jallouk, and E.R.F. Winter, "Single-Phase Transport Processes in the Closed Thermosyphon," Int. J. Heat Mass Transfer, Vol. 14 (7), pp. 869-887 (1971).
[15] G.S.H. Lock, and J.D. Kirchner, "Some Characteristics of the Inclined, Closed Tube Thermosyphon Under low Rayleigh Number Conditions," Int. J. Heat Mass Transfer, Vol. 35 (1), pp. 165-172 (1992).
[16] P. Bontoux, C. Smutek, B. Roux, and J.M. Lacroix, "Three Diamensional, Buoyancy- Driven Flows in Cylindrical Cavities with Differentially- Heated End Walls- I. Horizontal Cylinders," J. Fluid Mech. 169, pp. 211-227 (1986).
[17] G. S.H. Lock, and J.C. Han, "Buoyant Flow of Air in a Long, Square Section Cavity Aligned with the Ambient Temperature Gradient," J. Fluid 207, pp. 489-504 (1989).

Received July 21, 2004
Accepted November 1, 2004